Morphometric Features of Cells of Cervical Intraepithelial Neoplasia Using Computer Aided Image Analysis

Olaofe Olaejirinde Olaniyi [a*], Akinyemi Hezekiah Morakinyo [b] and Komolafe Akinwumi Oluwole [a]

[a] *Department Morbid Anatomy and Forensic Medicine, Obafemi Awolowo University Teaching Hospital, Ile-Ife, Osun State, Nigeria.*
[b] *Department Morbid Anatomy and Histopathology, Osun State University, Osogbo, Osun State, Nigeria.*

Authors' contributions

This work was carried out in collaboration among all authors. All authors read and approved the final manuscript.

Original Research Article

ABSTRACT

Aim: Our goal is to evaluate and compare the different cell morphometric parameters in the various categories of cervical intraepithelial neoplasia (CIN).
Study Design: We conducted a cross-sectional study of all cervical intraepithelial neoplasia identified in some areas of biopsies of cervical carcinomas.
Place and Duration of Study: The study was in the department of histopathology of LAUTECH Teaching Hospital, Osogbo from January 2006 to December 2015.
Materials and Methods: The histologic slides produced were scanned using CS2 APERIO digital slide scanner with standard settings. The scanned slides were then viewed using Qu Path-0.3.2 software. All areas of cervical intraepithelial neoplasia were selected. The perimeter, area,

_____

Corresponding author: E-mail: oolaofe @oauife.edu.ng;

maximum caliper, circularity, eccentricity, and the various measures of hematoxylin optic densities (OD) of the nucleus of the cells were measured. The cytoplasmic morphometric measurements and the nuclear-cell ratio were then estimated.

Results: Two cases of CIN 1, one case of CIN 2 and one case of CIN 3 were seen in the background of the eighty-seven cases of cervical carcinomas seen during the study period. A total of 5,935 cells were in the annotated regions with cervical intraepithelial neoplasia. The cells in CIN 1 area are 3,828, CIN 2 area has 1183 cells and CIN 3 areas has 924 cells. Cells of CIN 3 had higher average nuclei hematoxylin optic density (OD), nuclei hematoxylin OD standard deviation and maximum hematoxylin OD than cells of CIN 2 and CIN 1. Cells of CIN 1 have higher average cell area, cell perimeter, cell circularity and mean cytoplasm eosin OD compared to cells of CIN 2 and 3.

Conclusion: Computer-aided image analysis using Qu Path software can be very instrumental in differentiating the various categories of cervical intraepithelial neoplasia especially in fragmented biopsies.

1. INTRODUCTION

Cervical cancer is one of the most common cancers in women [1–4]. It is a deadly disease that can be easily prevented partly due to the relatively easy accessibility of the uterine cervix to direct visual inspection and tissue sampling. Although many approach, including computer-aided techniques [5–10], have been taken to improve prevention of cervical cancer, early detection and treatment of preneoplastic lesions remains very important in reducing the incidence of the malignant disease.

Cervical intraepithelial neoplasia (CIN) is a preneoplastic lesion that is detected in histopathological analysis of cervical biopsies usually taken from suspicious cervical lesions. The lesions are classified as cervical intraepithelial neoplasia I, II or III based on architectural changes in these preneoplastic lesions. The architectural changes used as criteria in the diagnosis of these lesions are based on the degree of deviation of the morphology from that of a normal cervical epithelium usually by the extent of loss of maturation of the epithelium. In a normal cervical epithelium, the nucleus reduces in size as the basally located cells get increasingly matured and move towards the more superficial part of the epithelium. This leads to a more prominent cytoplasm. The nucleus as they get smaller tend to have more tightly packed chromatin. In CIN, there is disruption in this orderly maturation such that the nuclear size may be relatively maintained for longer zones of the epithelium than normal.

Qu Path software is a tool that is able to objectively measure many parameters of the cell such as the size of nucleus, eccentricity of nucleus, circularity of the nucleus and size of cytoplasm. It has been used in numerous computer-aided image analysis to help to develop novel methods of tissue diagnosis in histopathology [11].

In this study, we aim to evaluate and compare the different morphometric parameters in the various grades of cervical intraepithelial neoplasia.

2. MATERIALS AND METHODS

We carried out a cross-sectional study of all cervical intraepithelial neoplasia identified in the background of biopsies of cervical carcinomas seen in the department of histopathology of LAUTECH Teaching Hospital, Osogbo from January 2006 to December 2015. The tissues had been fixed in formalin and then processed through varying grades of alcohol. The tissues were embedded in paraffin wax and sectioned with a microtome blade. The slides were stained with hematoxylin and eosin and then covered with a coverslip.

The slides produced were scanned using CS2 APERIO digital slide scanner with standard settings. The scanned slides were then viewed using Qu Path-0.3.2 software. All the areas of epithelium with cervical intraepithelial neoplasia were annotated and the digital images labelled accordingly. All areas of poorly processed tissues or with artefacts were excluded from the selection so as not to interfere with the cell detection process of the Qu Path software. All areas of carcinoma, necrotic tissue and stroma tissue were not annotated. The wand or brush tool was used for annotation and corrected

where appropriate. We ensured that the annotated areas were adjusted appropriately to focus only on the cells of cervical intraepithelial neoplasia.

The cell detection feature of the software was adjusted to the best setting to optimally detect the various parameters of the cell. The background nuclei radius was at 8μm, median filter radius at 0 μm, sigma at 1.5μm, minimum area at 10μm^2 and maximum area at 400 μm^2.

All areas of cervical intraepithelial neoplasia were selected. The perimeter, area, circularity, maximum caliper, eccentricity, and the various measure of hematoxylin optic densities (OD) of the nucleus of each of the cells were measured. The perimeter, area, circularity, maximum caliper, eccentricity, and the various measure of eosin optic densities (OD) of the cytoplasm of the cells were measured. The nuclear-cell ratio was then estimated.

The result of the analysis was exported to Microsoft excel and further analyzed using R

programming language in the Integrated Development Environment of R studio version 4.2.2. The charts were produced using ggplot 2 package.

3. RESULTS

Two cases of cervical intraepithelial neoplasia (CIN) 1, one case of CIN 2 and one case of CIN 3 were seen in the background of the 87 biopsies of cervical carcinomas seen during the study period. A total of 5,935 cells were in the annotated regions of the areas with cervical intraepithelial neoplasia. The cells in CIN 1 area are 3,828, CIN 2 area with 1183 cells and CIN 3 areas with 924 cells. Cells of CIN 3 had higher average nuclei hematoxylin optic density (OD), nuclei hematoxylin OD standard deviation and maximum hematoxylin OD than cells of CIN 2 and CIN 1 (Table 1). Cells of CIN 1 have higher average cell area, cell perimeter, cell circularity and mean cytoplasm eosin OD compared to cells of CIN 2 and 3 (Table 2). The other findings are presented in Figs. 2-13.

Table 1. Nucleus morphometry of cells of Cervical Intraepithelial Neoplasia (CIN) 1, 2 and 3 measured by Qu Path software

		Mean	Std. Deviation
Nucleus: Area (μm^2)	CIN 1	28.504673	16.7481572
	CIN 2	23.110567	12.6256707
	CIN 3	24.914338	12.6592042
Nucleus: Perimeter (μm)	CIN 1	23.879856	10.3624931
	CIN 2	21.066048	7.7905312
	CIN 3	22.113265	7.1022076
Nucleus: Circularity	CIN 1	.655960	.1731901
	CIN 2	.668570	.1542902
	CIN 3	.648424	.1543183
Nucleus: Max caliper (μm^2)	CIN 1	8.855958	3.4548989
	CIN 2	8.386449	3.3511882
	CIN 3	8.814949	3.0516825
Nucleus: Eccentricity	CIN 1	.797060	.1378980
	CIN 2	.840360	.1282616
	CIN 3	.841529	.1370498
Nucleus: Hematoxylin OD mean	CIN 1	.161715	.1674335
	CIN 2	.132986	.1025827
	CIN 3	.544126	.1955154
Nucleus: Hematoxylin OD std dev	CIN 1	.075724	.0393285
	CIN 2	.064185	.0300465
	CIN 3	.178243	.0659040
Nucleus: Hematoxylin OD max	CIN 1	.358842	.2432566
	CIN 2	.270479	.1589926
	CIN 3	.949386	.3241355

Table 2. General cell and cytoplasm morphometry of cells of Cervical Intraepithelial Neoplasia (CIN) 1, 2 and 3 measured by Qu Path software

		Mean	Std. Deviation
Cell: Area (μm^2)	CIN 1	107.875096	53.8573549
	CIN 2	77.002812	34.5602004
	CIN 3	101.016150	43.9311257
Cell: Perimeter (μm)	CIN 1	40.560050	10.6752952
	CIN 2	34.826565	8.5767641
	CIN 3	39.931627	8.8803362
Cell: Circularity	CIN 1	.787758	.0957274
	CIN 2	.775814	.0918125
	CIN 3	.786742	.0885546
Cell: Eccentricity	CIN 1	.705482	.1469791
	CIN 2	.744380	.1493767
	CIN 3	.739949	.1395490
Cytoplasm: Eosin OD mean	CIN 1	.639428	.1215800
	CIN 2	.399365	.0673399
	CIN 3	.610802	.0980901
Cytoplasm: Eosin OD std dev	CIN 1	.144066	.0645255
	CIN 2	.114861	.0373658
	CIN 3	.190082	.0479789
Nucleus/Cell area ratio	CIN 1	.273352	.0939665
	CIN 2	.300814	.0829177
	CIN 3	.248753	.0894503
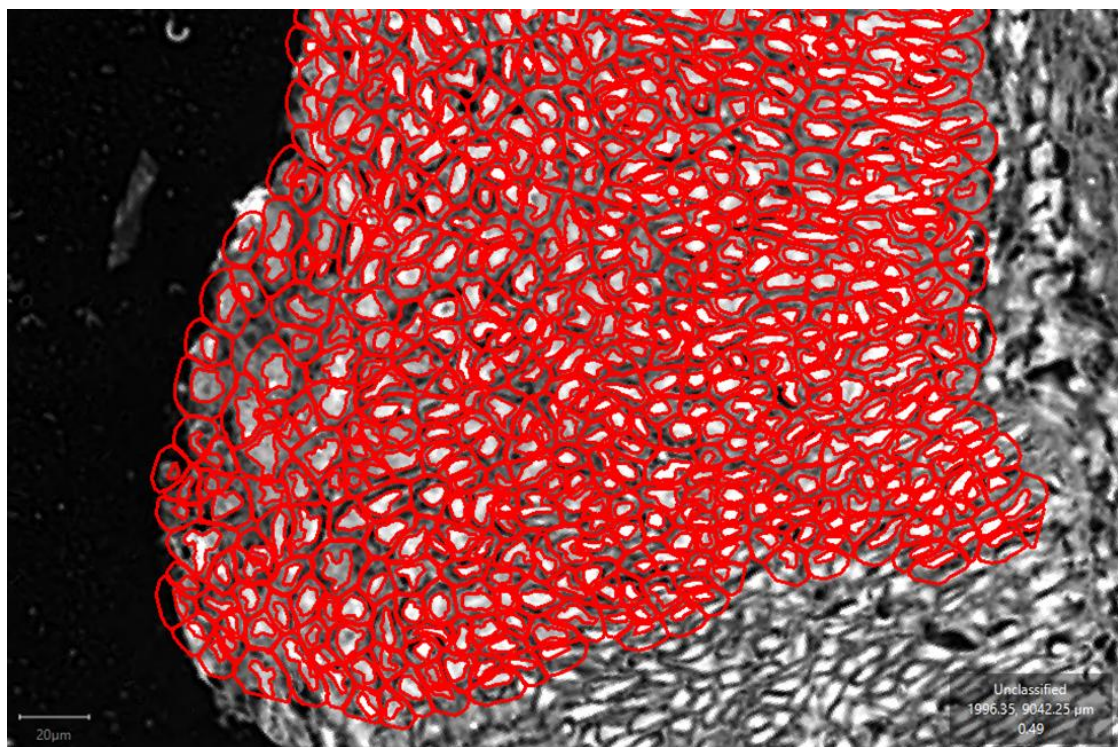
Fig. 1. Photomicrograph of nuclear and cytoplasmic membrane detection by Qu Path software
The photomicrograph shows detection of the nucleus and cytoplasmic membrane of cells of cervical intraepithelial neoplasia 3 in one of the annotated areas
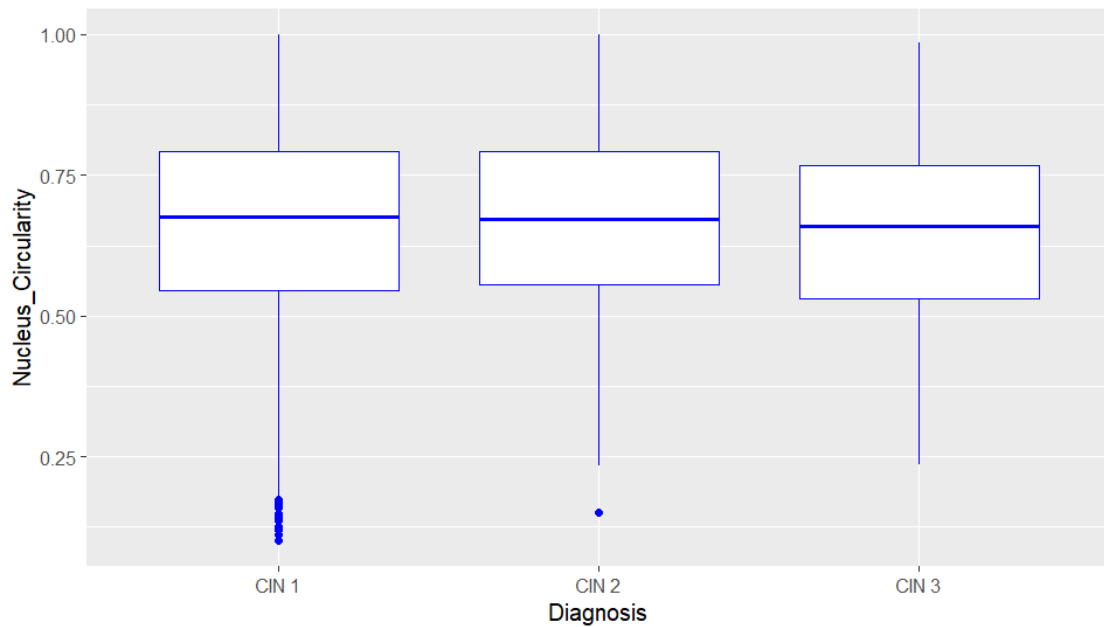
Fig. 2. Boxplot of nucleus circularity for the various CIN cells
The box-plot above shows similar distribution of the nuclear circularity in the various cervical intraepithelial neoplasia
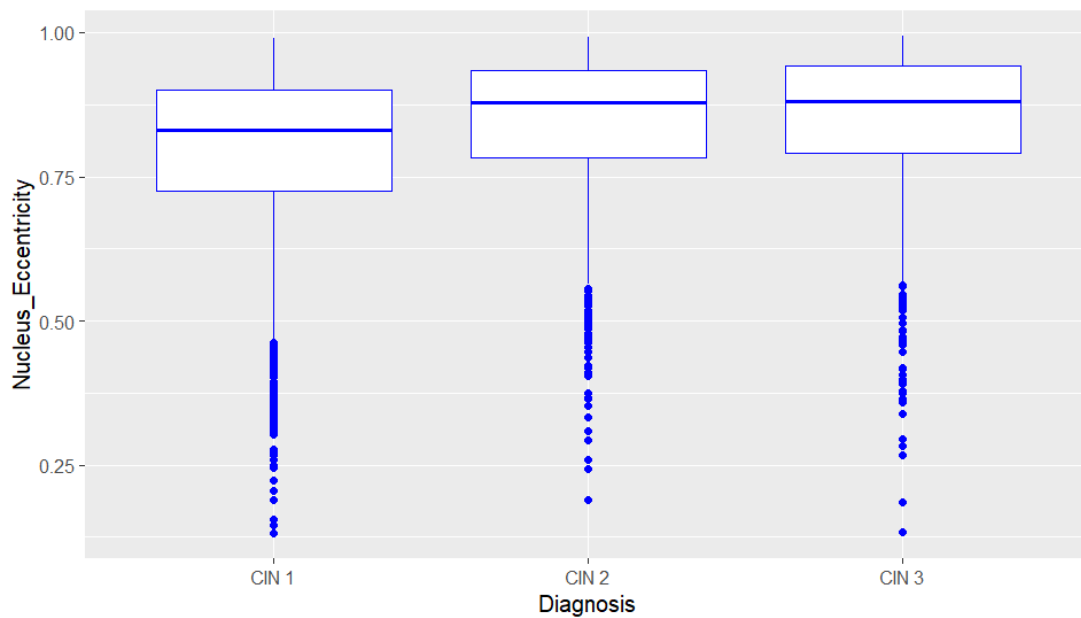

Fig. 3. Boxplot of nucleus eccentricity for the various CIN cells
The box-plot above shows a slight increase in the nuclei eccentricity of cells of CIN 2 and 3 but with significant overlap in the distribution of the three classes

4. DISCUSSION

Differentiating between the various categories of cervical epithelial neoplasia (CIN) is important in clinical practice as this has different management implications. The higher levels of dysplasia are managed more aggressively than the lower levels due to the higher risk of malignant transformation in the former. Our study shows some differences in the various cells of the categories of CIN. These can be eventually explored in the development of algorithms that can help to distinguish them using digital pathology [11,12].

Results from our work shows that cells of CIN 3 have higher hematoxylin stain intensity and higher variation in the staining intensity within a particular nucleus (Figs. 4 and 6). This is a measure of hyperchromatic and heterochromatic nature of the nucleus respectively. Epithelium of CIN 3 has almost or complete full thickness loss of maturation of the upwardly migrating basal cells from the lowermost layer of the epithelium.

In addition to this, they are known to have significant atypia with hyperchromatism being one of its major characteristics. The finding of higher hematoxylin intensity (more hyperchromatic nuclei) in CIN 3 by the software conforms to the previously known criterium [13]. This can be used in developing algorithms to help distinguish CIN 3 from the lower levels of dysplasia.
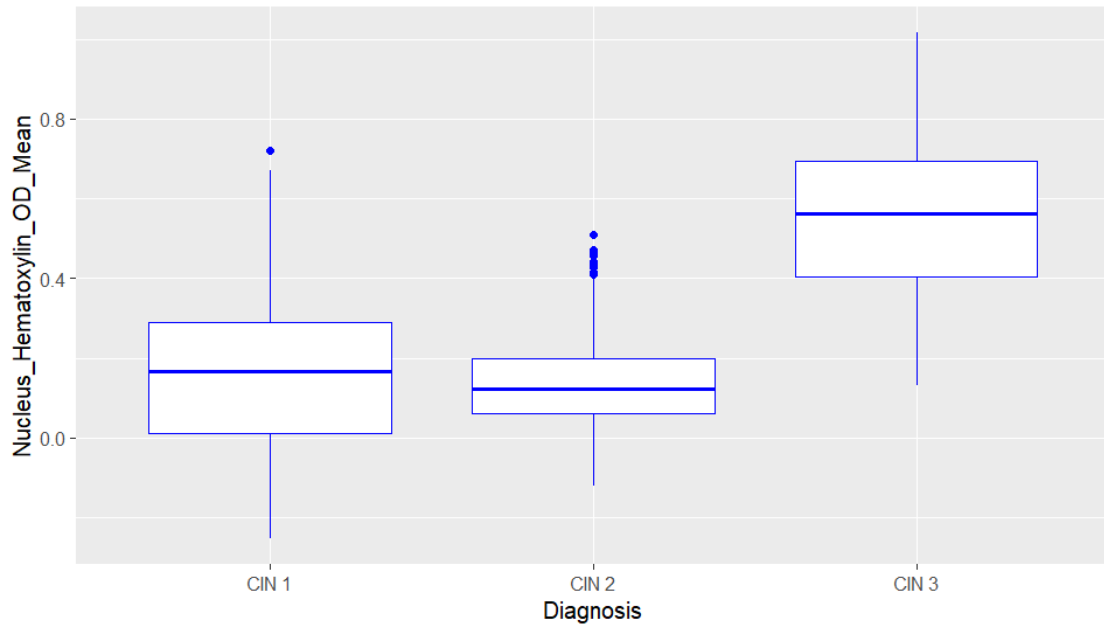
Fig. 4. Boxplot of mean nucleus hematoxylin OD for the various CIN cells
The box-plot above shows the distribution of mean hematoxylin optic density in cells of CIN 3 to be higher than that of cells of CIN 1 and CIN 2. (p<0.001)
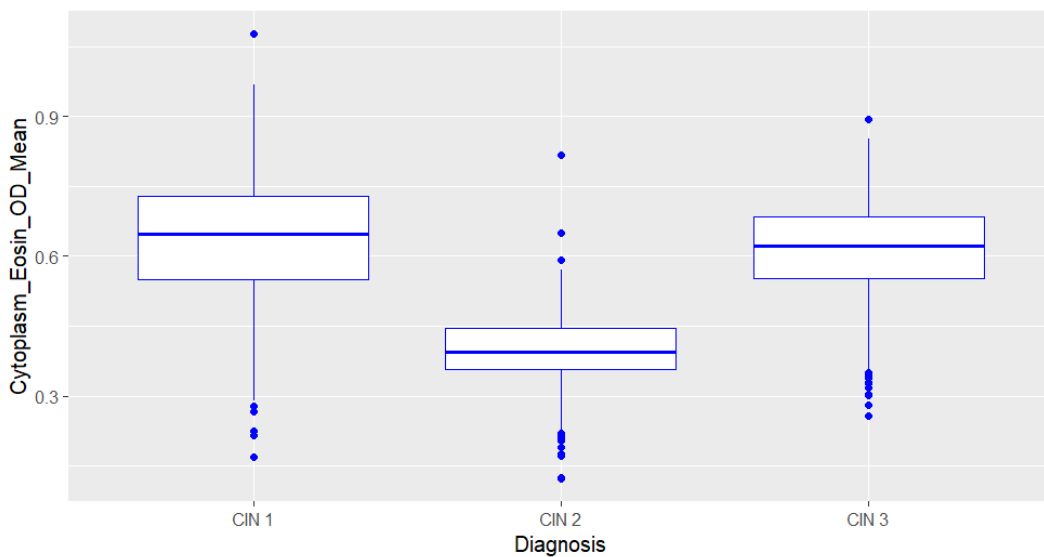

Fig. 5. Boxplot of mean cytoplasmic eosin OD for the various CIN
The box-plot above shows the mean eosin intensity distribution to be higher in CIN 1 cytoplasm compared to other cells. There is significant overlap of values of CIN 1 and CIN 3 cells
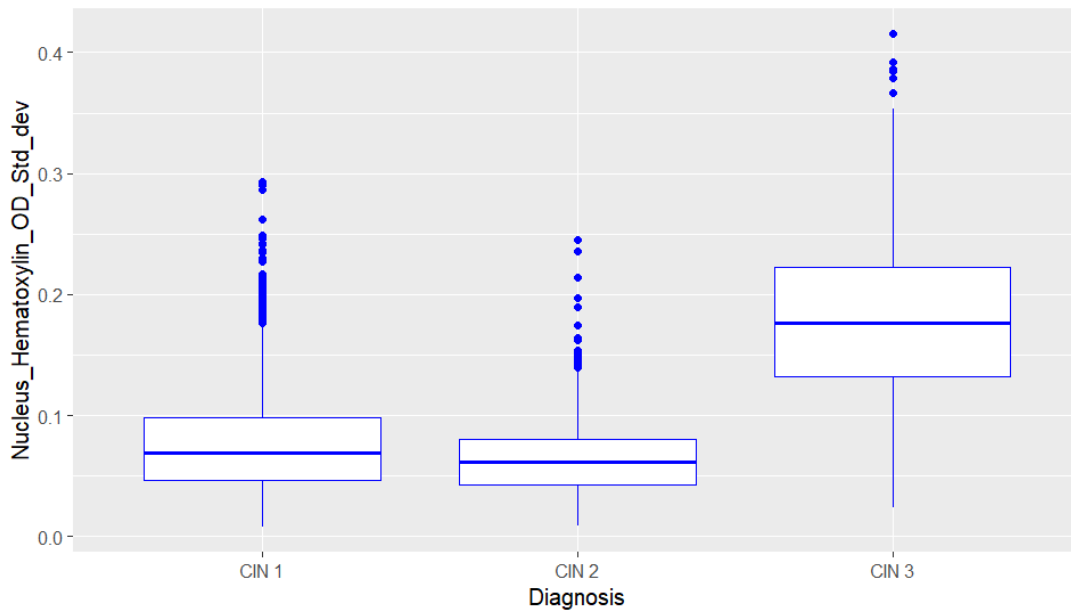
Fig. 6. Boxplot of standard deviation of nuclei hematoxylin for each type of CIN
The box-plot above shows that CIN 3 cells have more variable standard deviation (std dev), a measure of variation in hyperchromaticity of the nuclei, than cells of CIN 1 and 2
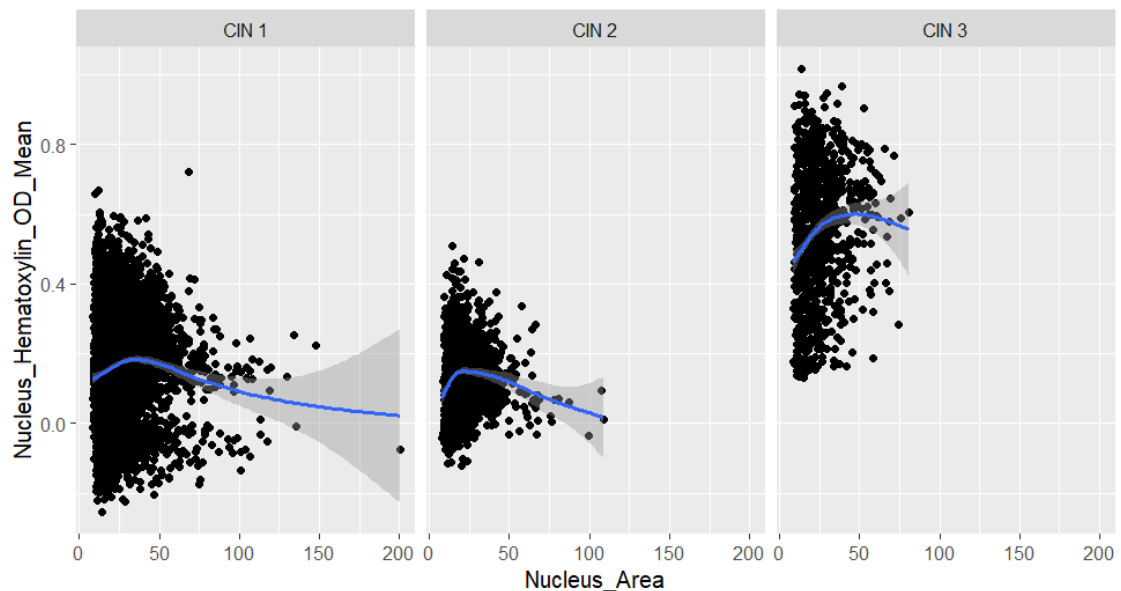

Fig. 7. Scatter diagram of relationship between nuclei hematoxylin and nucleus area
The relatively flat blue line suggests poor relationship between the degree of hematoxylin stain and size of the nucleus for all categories of CIN. (r = -0.003344036)

We observed that cells of CIN 1 have larger average size (cell area and perimeter) compared to cells of CIN 2 and 3 (Table 2). In normal epithelium, the cell and nuclear size reduces as the basal cells migrate upward. However, the reduction in nuclear size is more drastic and leads to the more superficial cells having reduced nucleo-cytoplasmic ratio. The larger size of the cells of CIN 1 may suggest that even though the cells of the higher categories of CIN have more prominent nuclei, the average size of their cells is less than that of CIN 1. This observation can be utilized in objectively distinguishing the higher grades of dysplasia or atypia from the lower grades.

The average cell circularity is observed to be higher in cells of CIN 1 than those of CIN 2 and 3 (Table 2). This is not unexpected as cells of higher grades of CIN are known to be more atypical and hence may be less circular as the degree of atypia increases [13]. It is however surprising that this was not noticed to be the case with measurements of nuclear circularity (Fig. 2). It might be due to the relatively pyknotic nature of the cells of the upper layers of CIN 1 or the atypia commonly caused by koilocytic atypia, thereby reducing any significant difference in nuclear circularity.
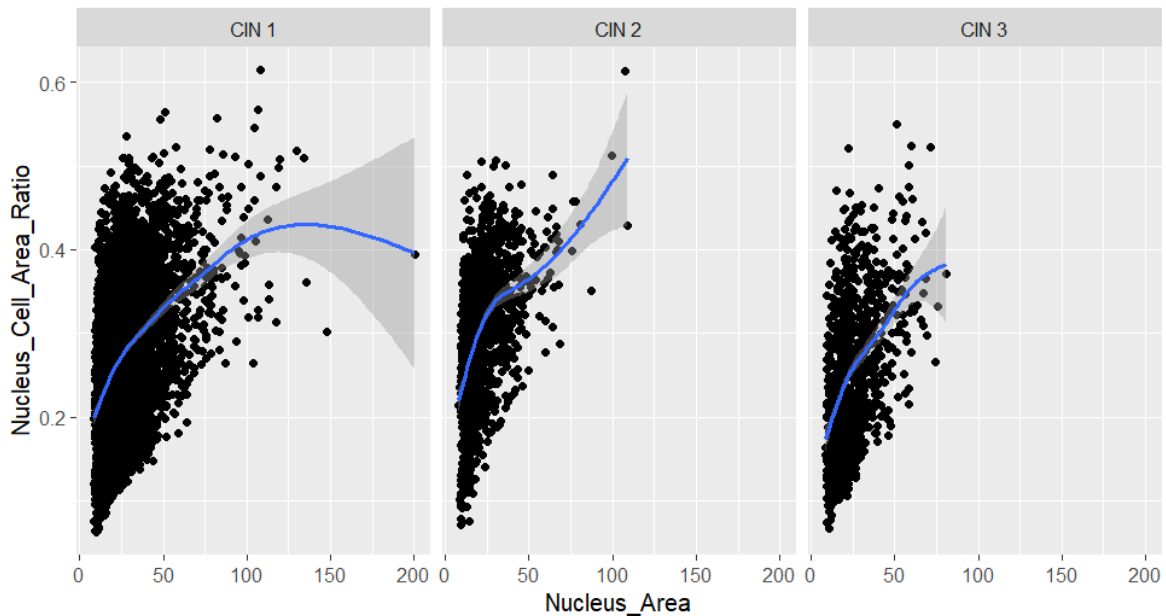
Fig. 8. Scatter diagram of relationship between nucleus-cell ratio and nucleus area for the various classes of cervical intraepithelial neoplasia
The box-plot above shows some degree of correlation between the Nucleus- Cell area ratio and Nucleus area for all the CIN. (Combined value of r = 0.4210578). The relationship appears stronger in CIN 3
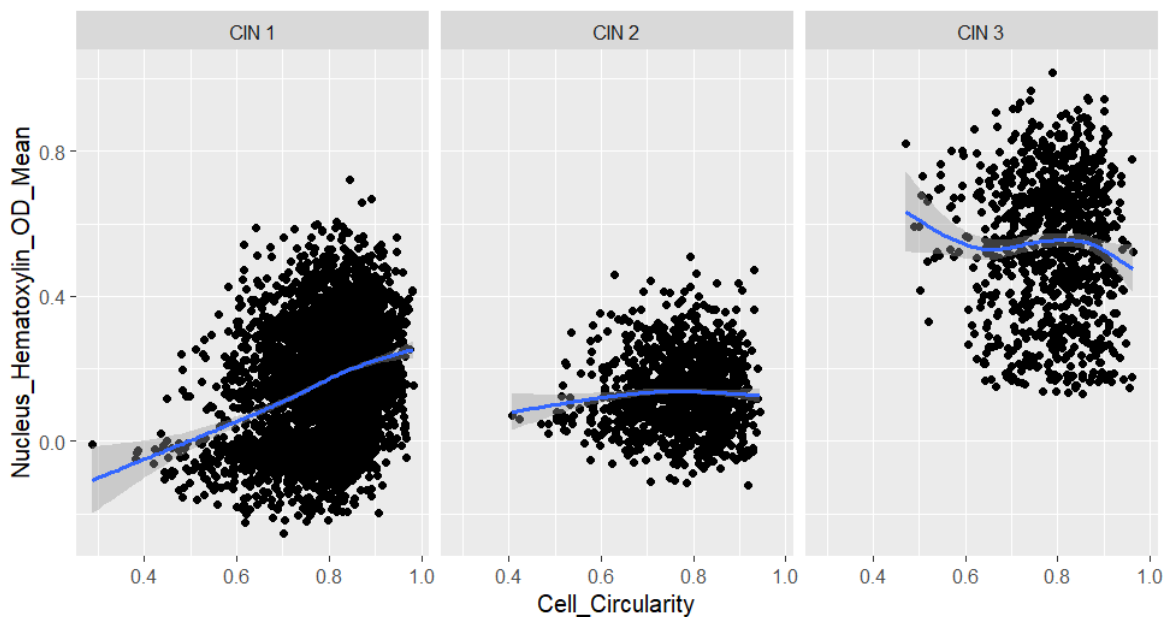

Fig. 9. Scatter diagram of relationship between nuclei hematoxylin and cell circularity
The figure demonstrates the relatively high hematoxylin intensity and the relatively higher values of cell circularity in the cells of CIN 3
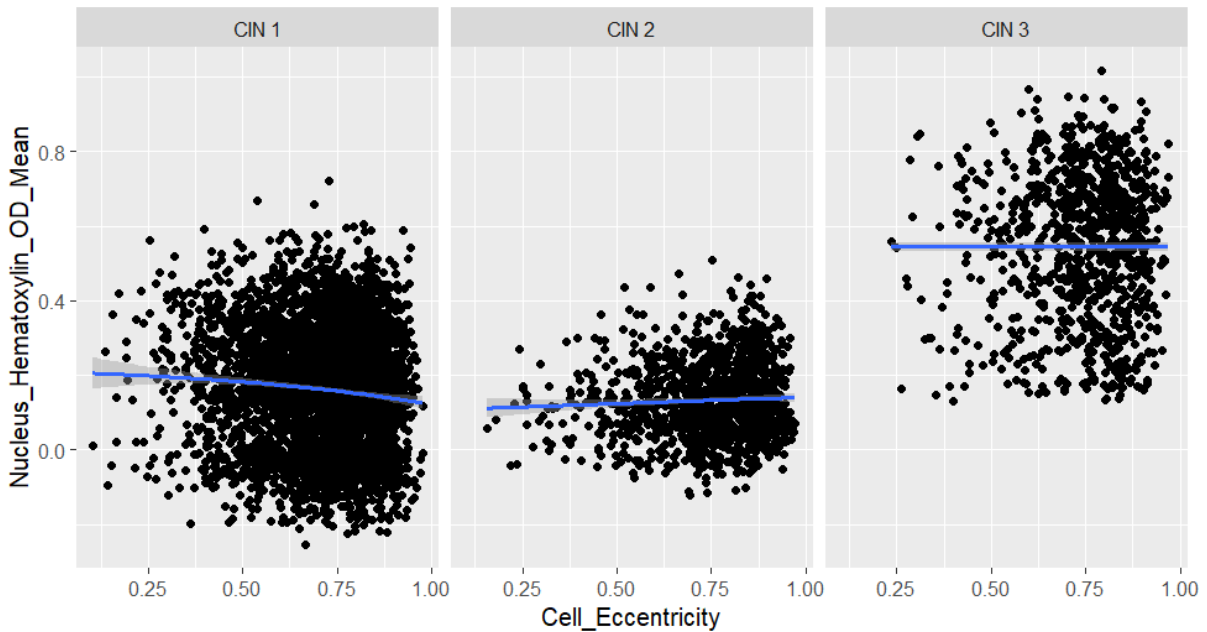
Fig. 10. Scatter diagram of relationship between mean nuclei hematoxylin OD and cell eccentricity
The relatively flat blue line shows that there is no meaningful relationship between nuclei hematoxylin OD and cell eccentricity (r = -0.003670447)
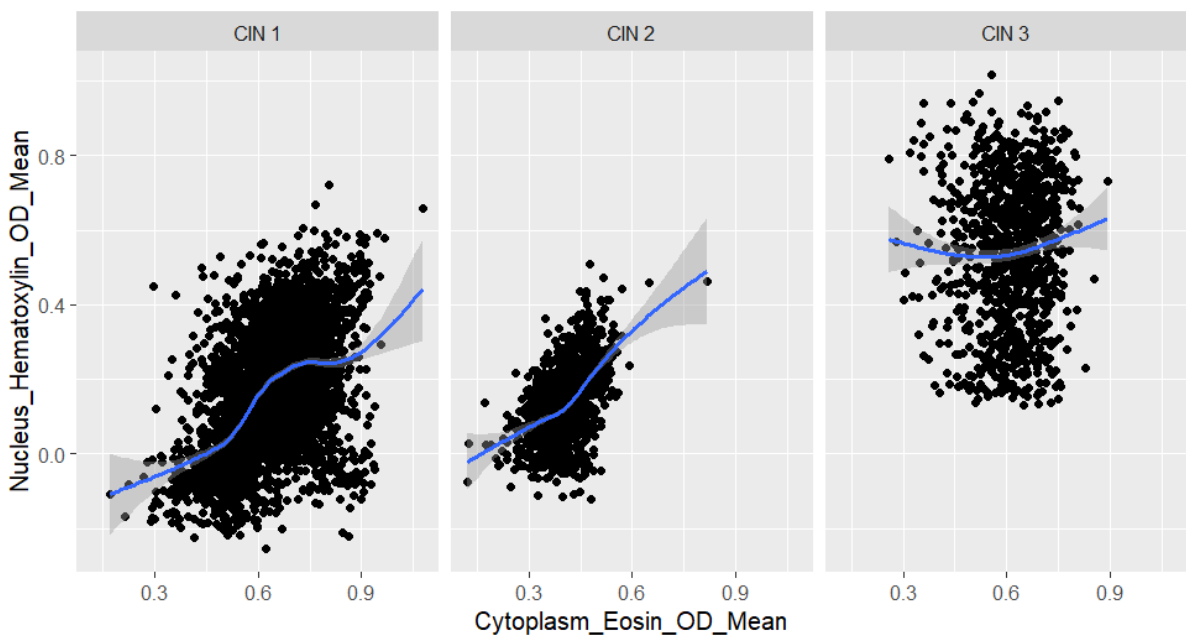

Fig. 11. Scatter diagram of relationship between nuclei hematoxylin and cytoplasmic eosin
This scatter diagram of CIN 1, 2 and 3 shows the high mean hematoxylin OD of the nucleus in CIN3. There appears to be a weak relationship between the intensity of nuclei hematoxylin and cytoplasmic eosin (r= 0.3300845). The relationship appears stronger in CIN 1 and 2 compared to CIN 3

The cytoplasmic eosin stain for cells of CIN 1 was seen to be much higher than cells of CIN 2 and 3 (Table 2 and Fig. 5). Since keratin is eosinophilic, the intensity of eosin stain can be safely used as an index of keratin production. As the epithelial cells get more dysplastic, they reduce their formation of keratin in the cytoplasm. However, the higher eosinophilic

intensity in the cells of CIN 3 compared to CIN 2 may be due to the higher rate of dyskeratosis in epithelium with CIN 3.

The nuclei of cells of CIN 2 and 3 were observed to be more eccentric than cells of CIN 1. This conforms to previously held notion as cells of higher grades of CIN are known to be more

atypical. Nuclear eccentricity is one of the features of atypia that these cells are known to have [13]. However, because of the significant overlap in the measurements of the nuclear eccentricity in all the three categories of CIN, it might be a weaker factor in differentiating these entities. It might have a role to play in the use of multifactorial algorithms.
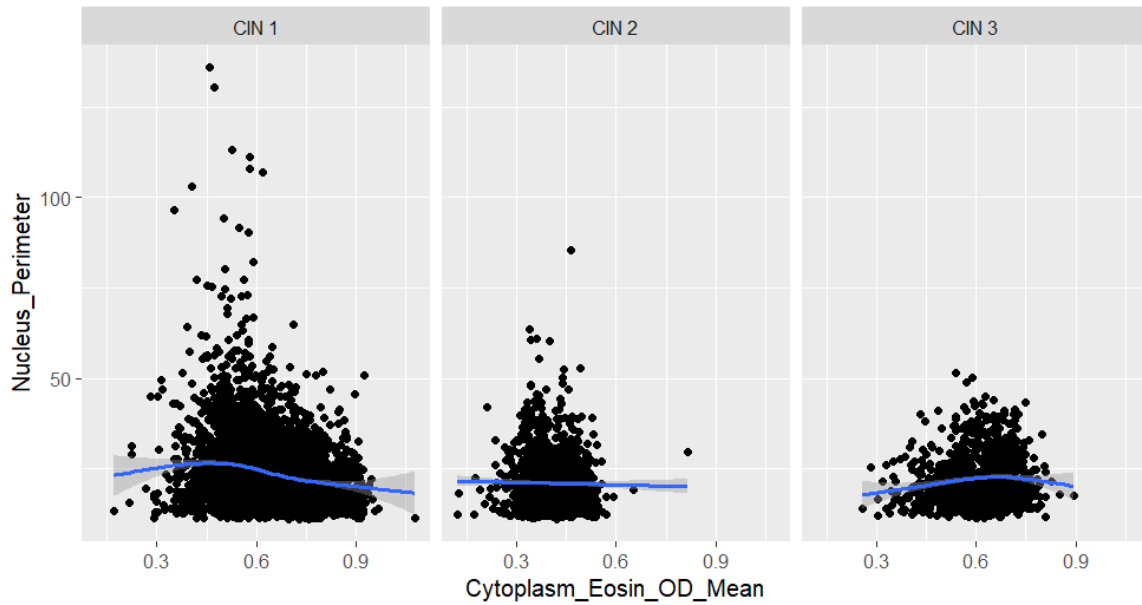

Fig. 12. Scatter diagram of relationship between nuclei perimeter and cytoplasmic eosin
There is no relationship between the perimeter of the nucleus and mean eosin density for CIN 1, 2 and 3 (r = -0.03374789)
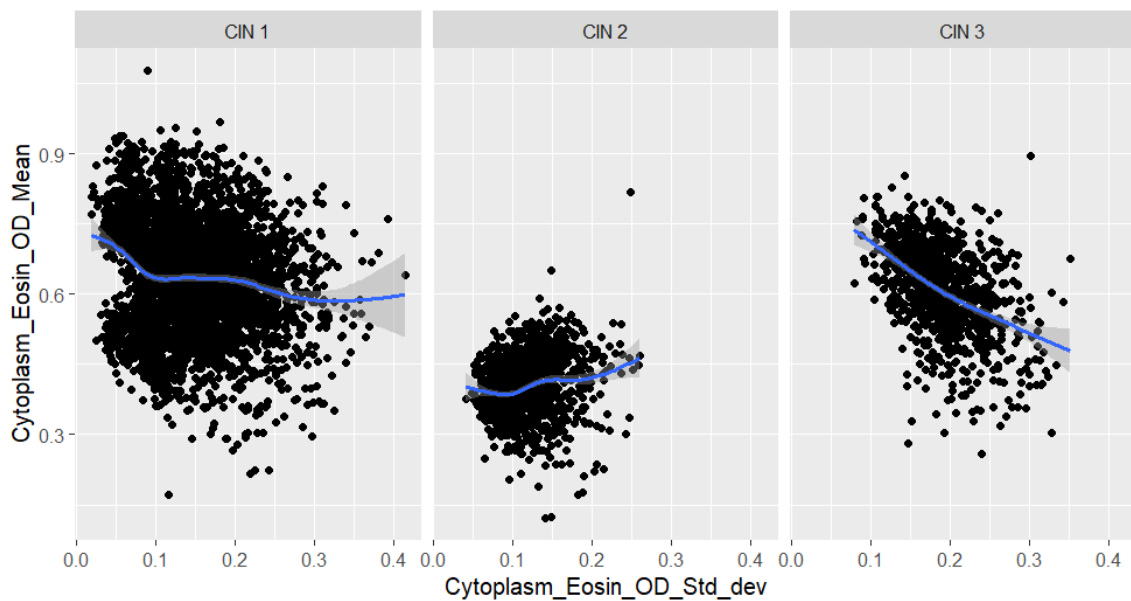

Fig. 13. Scatter diagram of relationship between mean cytoplasmic eosin density and its variability (standard deviation) for each cell
There is generally no relationship between eosin intensity and its variability (r = 0.01194283). There seems to be a negative relationship between eosin intensity and its variability in CIN 3

Although one might be tempted to think that cells of CIN will have higher hematoxylin intensity as the size of the nuclei increases, this was not found to be the case in our study. We found that the nuclear size does not increase with hematoxylin intensity for any of the categories of CIN (Fig. 7). The nucleus area of CIN 3 cells was however found to be less variable in Fig. 7.

The nuclear size was seen to have some degree of correlation with nucleocytoplasmic ratio as seen in Fig. 8. It is a well-known fact that more atypical cells have higher nuclear size and higher nucleo-cytoplasmic ratio. The Nucleus-Cell area can be taken to represent the nucleocytoplasmic ratio. The relationship seems to be stronger in cells of CIN 3 as shown by the blue lines in Fig. 8.

We observed some degree of correlation between the intensity of nucleus hematoxylin and intensity of cytoplasmic eosin. This seems to be more prominent in CIN 1 and 2 and less so in CIN 3 (Fig. 11). We had earlier observed the higher hematoxylin intensity and lower eosin intensity in CIN 3 cells (Figs. 4, 5 and 6). Hence the reduced presence of keratin in the more hyperchromatic and more atypical CIN 3 cells may partly account for the low correlation.

We observed there is no relationship between the nuclear size as measured by the nuclear perimeter and the cytoplasmic eosin intensity as measured by the cytoplasmic eosin optic density (Fig. 11). This conforms to other findings in this study that have failed to show significantly larger nuclear size or cytoplasmic keratin in the higher grades of cervical intraepithelial neoplasia.

We noticed there is more negative relationship between cytoplasmic eosin (a measure of keratin) and its variability in cells of CIN 3 compared to CIN 1 and 2. This suggests that in cells of CIN 3, as the cytoplasmic keratin reduces, it becomes more uniform in the cytoplasm. This observation may be important in developing algorithms for identifying the CIN 3 epithelium.

5. CONCLUSION

Computer-aided image analysis using Qu Path software can be very instrumental in differentiating the various categories of cervical intraepithelial neoplasia especially in fragmented biopsies. Cells of CIN 3 have higher hematoxylin stain intensity and higher variation in the staining intensity within a particular nucleus. Cells of CIN 1 have larger average size (cell area and perimeter) compared to cells of CIN 2 and 3. The average cell circularity is observed to be higher in cells of CIN 1 than those of CIN 2 and 3. The cytoplasmic eosin stain for cells of CIN 1 was seen to be much higher than cells of CIN 2 and 3.

AVAILABILITY OF DATA AND MATERIALS

The data on all the measurements for each of the 3,828 CIN 1 cells, 1183 CIN 2 cells and 924 CIN 3 cells are available on request.

CONSENT

It is not applicable.

ETHICAL APPROVAL

Ethical approval was obtained from the local ethics and research review board.

COMPETING INTERESTS

Authors have declared that no competing interests exist.

REFERENCES

1.   Cervical cancer [Internet]. Available:https://www.who.int/health-topics/cervical-cancer Access on 2023 Mar 16
2.   Arbyn M, Weiderpass E, Bruni L, Sanjosé S de, Saraiya M, Ferlay J, et al. Estimates of incidence and mortality of cervical cancer in 2018: A worldwide analysis. Lancet Glob Health. 2020;8(2):e191–203.
3.   Bray F, Ferlay J, Soerjomataram I, Siegel RL, Torre LA, Jemal A. Global cancer statistics 2018: GLOBOCAN estimates of incidence and mortality worldwide for 36 cancers in 185 countries. CA Cancer J Clin. 2018;68(6):394–424.
4.   Farnsworth A, Roberts JM, Garland SM, Crescini J, Kaldor JM, Machalek DA.

Detection of high-grade cervical disease among women referred directly to colposcopy after a positive HPV screening test varies with age and cytology findings. Int J Cancer. 2020;147(11):3068–74.

5. Conceição T, Braga C, Rosado L, Vasconcelos MJM. A review of computational methods for cervical cells segmentation and abnormality classification. Int J Mol Sci. 2019;20(20): 5114.

6. William W, Ware A, Basaza-Ejiri AH, Obungoloch J. A review of image analysis and machine learning techniques for automated cervical cancer screening from pap-smear images. Comput Methods Programs Biomed. 2018;164:15–22.

7. Hu L, Bell D, Antani S, Xue Z, Yu K, Horning MP, et al. An observational study of deep learning and automated evaluation of cervical images for cancer screening. J Natl Cancer Inst. 2019;111(9):923–32.

8. Hou X, Shen G, Zhou L, Li Y, Wang T, Ma X. Artificial intelligence in cervical cancer screening and diagnosis. Front Oncol. 2022;12:851367.

9. Bora K, Chowdhury M, et al. Automated classification of pap smear images to detect cervical dysplasia. Comput Methods Programs Biomed. 2017;138: 31–47.

10. Sompawong N, Mopan J, Pooprasert P, Himakhun W, Suwannarurk K, Ngamvirojcharoen J, et al. Automated pap smear cervical cancer screening using deep learning. Annu Int Conf IEEE Eng Med Biol Soc. 2019;2019:7044–8.

11. Herrington CS, Poulsom R, Pillay N, Bankhead P, Coates PJ. Recent advances in pathology: the 2022 annual review issue of the journal of pathology. J Pathol. 2022;257(4):379–82.

12. Bankhead P. Developing image analysis methods for digital pathology. J Pathol. 2022;257(4):391–402.

13. Fischer EG. Nuclear morphology and the biology of cancer cells. Acta Cytol. 2020;64(6):511–9.